CHEMISTRY
A EUROPEAN JOURNAL

DOI: 10.1002/chem.201101635

A Cyclodextrin-Based Nanoassembly with Bimodal Photodynamic Action

Noufal Kandoth,[a] Elisa Vittorino,[a] Maria Teresa Sciortino,[b] Tiziana Parisi,[b] Ivana Colao,[b] Antonino Mazzaglia,*[c] and Salvatore Sortino*[a]

Abstract: We have developed a supramolecular nanoassembly capable of inducing remarkable levels of cancer cell mortality through a bimodal action based on the simultaneous photogeneration of nitric oxide (NO) and singlet oxygen ($^1O_2$). This was achieved through the appropriate incorporation of an anionic porphyrin (as $^1O_2$ photosensitizer) and of a tailored NO photodonor in different compartments of biocompatible nanoparticles based on cationic amphiphilic cyclodextrins. The combination of steady-state and time-resolved spectroscopic techniques showed the absence of significant intra- and interchromophoric interaction between the two photoactive centers embedded in the nanoparticles, with consequent preservation of their photodynamic properties. Photodelivery of NO and $^1O_2$ from the nanoassembly on visible light excitation was unambiguously demonstrated by direct and real-time monitoring of these transient species through amperometric and time-resolved infrared luminescence measurements, respectively. The typical red fluorescence of the porphyrin units was essentially unaffected in the bichromophoric nanoassembly, allowing its localization in living cells. The convergence of the dual therapeutic action and the imaging capacities in one single structure makes this supramolecular architecture an appealing, multifunctional candidate for applications in biomedical research.

Keywords: cyclodextrins · drug delivery · imaging agents · nitric oxide · phototherapeutic agents · singlet oxygen

Introduction

Bimodal therapies aim to exploit either additive or synergistic effects arising from the generation of two active species in the same region of space, with the final goal of maximizing the therapeutic efficacy. The site of action, timing, and dosage of the delivered species play key roles in determining the therapeutic outcome.[1] Light is a highly orthogonal trigger for the rapid introduction of therapeutic agents in a desired bio-environment with the potential for precise control over all the above factors and the additional advantage of not affecting important physiological parameters such as temperature, pH, and ionic strength.[2] These properties make phototherapeutic agents a powerful arsenal for treating cancer diseases in a noninvasive way,[3] avoiding the possible complications of surgery.[4]

Nitric oxide (NO) is one of the most appealing and intensely studied molecules in the fascinating realm of the biomedical sciences.[5] Besides its pivotal role in the maintenance and bioregulation of vital functions,[6] NO has recently stimulated an upsurge of interest because of its promising anticancer activity.[7] This exciting discovery has made the development of new strategies and methods for NO photodelivery a hot topic with the intriguing prospect of tackling cancer diseases.[8] In this regard, the use of NO in conjunction with other anticancer species is highly desirable for effective therapeutic action.[9]

Singlet oxygen ($^1O_2$) is the best-known phototherapeutic agent and its role in photodynamic therapy (PDT) is well established.[10] In PDT, the cytotoxic $^1O_2$ is generated by photoinduced energy transfer between the lowest excited triplet state of a suitable photosensitizer (e.g., a porphyrin or phthalocyanine) and nearby molecular oxygen.[11] Unlike other reactive oxygen species (that is, hydrogen peroxide and superoxide radical), $^1O_2$ is not consumed by enzymes such as catalase and superoxide dismutase produced by cancer cells.[12] Furthermore, PDT is not affected by multiple drug resistance, overcoming the major problems faced in chemo- and radiotherapy.[13] The combination of $^1O_2$ with NO therefore in principle represents an ideal strategy for bimodal treatments. On the basis of these considerations the objective of this work was to develop a multifunctional molecular ensemble capable of simultaneous photogeneration

[a] N. Kandoth, Dr. E. Vittorino, Prof. S. Sortino
Laboratory of Photochemistry
Department of Drug Sciences, Viale Andrea Doria 6
95125 Catania (Italy)
Fax: (+39) 095 580138
E-mail: ssortino@unict.it

[b] M. T. Sciortino, T. Parisi, I. Colao
Dipartimento di Scienze della Vita
Sezione di Scienze Microbiologiche Genetiche e Molecolari
Università di Messina, Salita Sperone, 98166 Messina (Italy)

[c] Dr. A. Mazzaglia
Istituto per lo Studio dei Materiali Nanostrutturati, ISMN-CNR
c/o Dipartimento di Chimica Inorganica Analitica e Chimica Fisica
Università di Messina, Salita Sperone, 98166 Messina (Italy)
Fax: (+39) 090 393756
E-mail: antonino.mazzaglia@ismn.cnr.it

of $^1O_2$ and NO and offering imaging capacities in living cells.

Nanotechnology offers enormous opportunities for the construction of effective delivery vehicles.[14] In the case of photoactivated compounds, three of the most important criteria that a carrier system would meet are: 1) biocompatibility, 2) cell-penetrating properties, and 3) preservation of the photodynamic activity of the photosensitizer.

Cyclodextrins (CDs) are water-soluble oligosaccharides well-known for the formation of host–guest inclusion complexes with a range of substrates.[15] Appropriate functionalization of the primary, secondary, or both sides of CDs leads to intriguing derivatives with amphiphilic character, able to self-organize in a variety of assemblies such as micelles, vesicles, and nanoparticles[16] with great potential in drug delivery.[17] Previously, we prepared and characterized heterotopic colloidal nanoparticles (NPs) based on the cationic amphiphilic CD **1** (Scheme 1), which is capable of trapping the oppositely charged porphyrin **2**, mainly through electrostatic interactions. The NPs have hydrodynamic radii ranging from ≈140 to ≈1000 nm, depending on the porphyrin loading.[18] We also showed that such NPs are promising vehicles for photodynamic therapy, because they combine low immunogenic activity, high capability to convey photosensitizers into tumor cells, and excellent levels of cell mortality upon light irradiation, due to effective photogeneration of $^1O_2$.[19] In addition, we demonstrated that the porphyrin units are not hosted in the interiors or vicinities of the CD cavities, offering the opportunity to exploit the empty cages in the CD-based NPs for the accommodation of additional guests.[20] In the wake of these promising results and motivated by our ongoing interest in developing NO photoreleasing systems,[21] here we report a fluorescent supramolecular nanoassembly capable of photo-deactivating cancer cells through a bimodal action due to the simultaneous generation of $^1O_2$ and NO under visible light excitation conditions (Scheme 1).

Results and Discussion

When CD **1** and the anionic porphyrin **2** are mixed together at a molar ratio of approximately 50:1, spontaneous formation of amphiphilic NPs approximately 300 nm in diameter is observed, according to our previous results.[18] Under these experimental conditions, the porphyrin is mainly entangled as the monomeric form, which is responsible for the $^1O_2$ generation (***a*** and ***b*** in Figure 1).

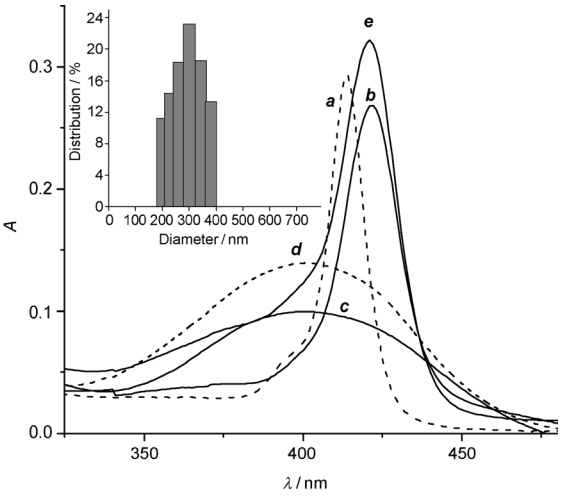

Figure 1. Absorption spectra (phosphate buffer, 10 mM, pH 7.4) of **2** (***a***) in the absence and (***b***) in the presence of CD **1**, (***c***) of **3** in the presence of CD **1**, (***d***) of the model compound **4** , and (***e***) of **2**+**3** in the presence of CD **1**. [**1**] = 40 μM, [**2**] = 0.8 μM, [**3**] = 10 μM, T = 25 °C, cell path = 1 cm. The inset shows the size distribution of the bichromophoric nanoassembly obtained by dynamic light scattering measurements.

To introduce an appropriate NO photoreleaser within these NPs, we designed and synthesized compound **3**

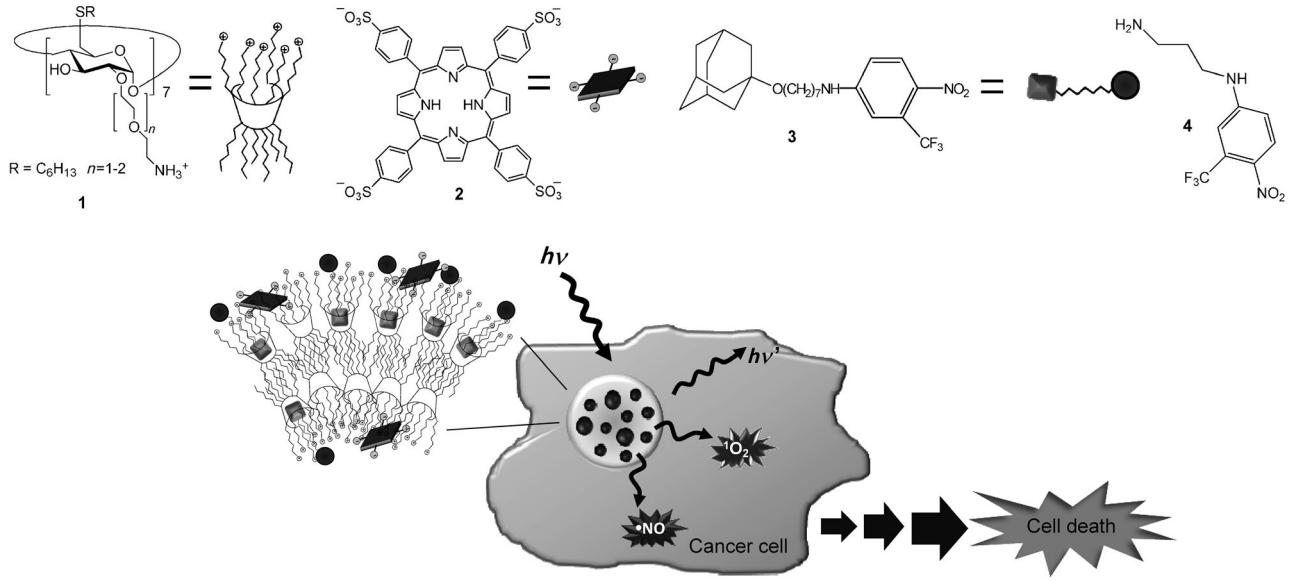

Scheme 1. Idealized view of the photoactive CD-based bichromophoric nanoassembly.

(Scheme 1), in which a commercial nitroaniline derivative and an adamantane appendage are joined together through an alkyl spacer. We have discovered the nitroaniline derivative to be a suitable NO photodonor[22] because it satisfies several prerequisites for bio-applications. In this compound, the twisted conformation of the nitro group with respect to the aromatic plane is crucial for the NO photorelease. However, it has been shown that incorporation of this chromophore within constrained environments, such as β-CD cavities[23] or densely packed vesicles,[24] can lead to partial planarization of the nitro group with consequent dramatic modification of the NO photoreleasing properties. With this in mind, the rationale behind the design of compound **3** was i) that the adamantane, a well-known and effective guest for β-CD,[25] would be expected to occupy the empty cavities in NPs based on CD **1**,[26] and ii) that use of an alkyl spacer of appropriate length should further encourage the binding of **3** with the NPs through cooperative hydrophobic interchain interactions involving the alkyl branches of CD **1**. It was envisaged that these effects should leave the nitroaniline chromophore mainly exposed to an aqueous environment, preserving the out-of-plane geometry and consequently the NO photoreleasing capacity. The validity of our design is demonstrated by the absorption spectra shown in Figure 1. Compound **3** is insoluble in aqueous solution. On the other hand, it becomes fairly soluble in the presence of the NPs based on CD **1**, as shown by the appearance of the characteristic absorption of the nitroaniline chromophore in the visible region (spectrum ***c***). These absorption features are basically the same as those exhibited by the water-soluble model compound **4** in the absence of NPs (spectrum ***d***). Because the energy of the visible absorption band is very sensitive both to microenvironment polarity and to changes in the geometry of the nitro group,[24] the absence of any significant spectral shift is highly consistent with the photoactive core being mainly exposed to an aqueous environment.

The bichromophoric nanoassemblies were prepared by loading the CD-based NPs with **2** and **3** at the appropriate molar ratio. The spectral characteristics observed (***e*** in Figure 1) match the profile obtained by summing the spectra of the NPs loaded with the individual chromophores **2** or **3** (***b*** and ***c*** in Figure 1) fairly well, with an experimental uncertainty of approximately 15% (in absorbance values). This confirms their concurrent presence within the NPs and the absence of relevant interactions with one another in the ground state. Moreover, the unaltered position of the maximum of the Soret band of **2** indicates that the presence of compound **3** does not induce any rearrangement (i.e., displacement/aggregation) of the porphyrins. This might be the consequence of different affinities of the two components for different binding sites in the NPs, consistently with the idealized view illustrated in Scheme 1.

Dynamic light scattering measurements showed the mean diameter of the bichromophoric nanoassemblies to be approximately 300 nm (Figure 1, inset), a value similar to that already reported for the NPs loaded with **2** alone at the same molar ratio.[18] This is consistent with the uncharged nature of compound **3**, which does not influence the charge balance between the anionic **2** and the cationic CD **1**. Such a balance has been demonstrated to be critical in driving porphyrin reorganization and promoting the fusion of the amphiphilic NPs into large aggregates of several hundreds of nanometers.[18]

The entangling of the monomeric porphyrin within the CD-based NPs results in a significant redshift of its typical dual band fluorescence emission with negligible changes in the fluorescence quantum yield (Figure 2A).[27] Interestingly, these emission properties were only slightly affected in the case of the bichromophoric nanoassembly, ruling out any intramolecular quenching (i.e., photoinduced electron-transfer) of the excited porphyrin by the NO photodonor. It is also worth noting that the positions of the two emission bands were independent of the excitation energy (data not shown), suggesting the presence in the nanoassembly mainly

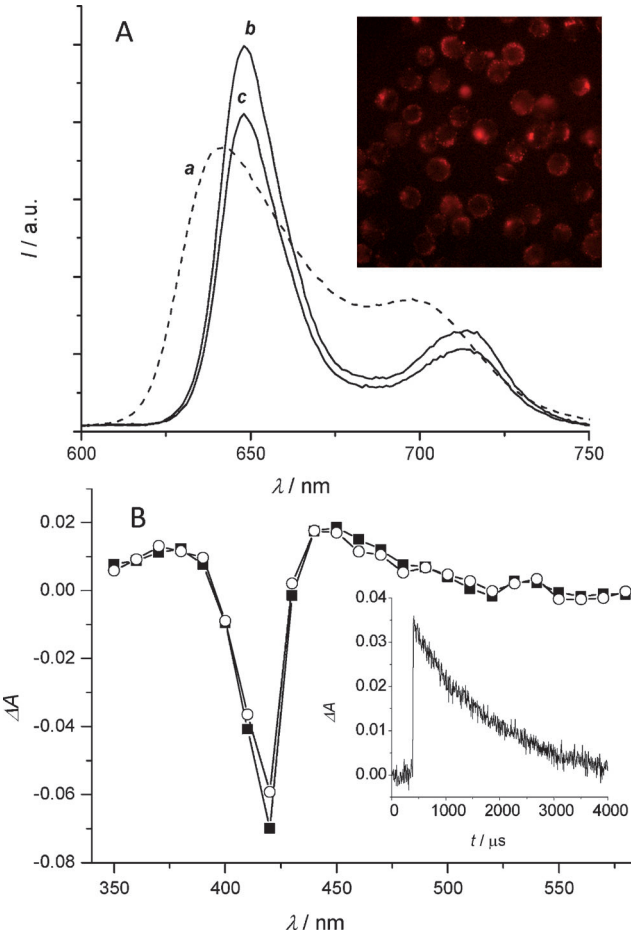

Figure 2. A) Fluorescence emission spectra (λ_{exc} = 440 nm) of **2** (***a***) in the absence and (***b***) in the presence of CD **1**, and (***c***) of **2**+**3** in the presence of CD **1**; the inset shows a representative microscopy image of HeLa cancer cells incubated with the bichromophoric nanoassembly for 1 h at 37 °C. B) Transient absorption spectra observed upon laser excitation (532 nm) of Ar-saturated CD **1** solution loaded with **2** (■) and **2**+**3** (○), recorded 0.1 μs after the laser pulse. Each point was obtained by signal averaging of 10 traces. The inset shows the decay trace monitored at 450 nm. E_{532} ≈ 12 mJ per pulse. Phosphate buffer (10 mM, pH 7.4), [**1**] = 40 μM, [**2**] = 0.8 μM, [**3**] = 10 μM, T = 25 °C.

of a single population of fluorophores (i.e., the monomeric form). The preservation of the fluorescence properties of the porphyrins under these experimental conditions represents a great advantage for mapping the nanoassembly in living cells. The inset of Figure 2A shows a representative optical image recorded in fluorescence mode after incubation of the bichromophoric NPs with HeLa tumor cells. This clearly represents the internalization of the supramolecular system in the cell compartment and shows that the localization takes place mainly at the cytoplasmatic level.

The excited triplet state of the porphyrin is the key intermediate for the photosensitization of $^1O_2$ and its effective generation is thus crucial for the photodynamic action.[11] Figure 2B shows the characteristic triplet absorption of **2** when entangled within the NPs in the absence and in the presence of the NO photodonor **3**. Because the two samples were optically matched at the excitation wavelength, the intensity of the transient absorption is directly related to the triplet quantum yield. The comparable values obtained for the two samples indicate that the triplet state of the porphyrin is still populated efficiently in the bichromophoric nanoassembly. Furthermore, the monoexponential decay of the triplet with a lifetime of approximately 1500 μs (inset, Figure 2B), which is the same as that observed in the absence of **3**,[19] indicates that no quenching by the NO photodonor occurs. Note that the observed lifetime is much longer than that of the free porphyrin in aqueous medium in the absence of NPs (ca. 200 μs),[19] ruling out any exit dynamics of the porphyrin triplet from the nanoassembly on this timescale.

The most convenient method for testing the suitability of the nanoassembly for photogeneration of NO and $^1O_2$ is the real-time monitoring of these transient species. To this end, an ultrasensitive NO electrode was used to detect NO concentrations by an amperometric technique, whereas time-resolved infrared luminescence was employed to monitor the typical phosphorescence of $^1O_2$ at 1270 nm.[28] Figure 3 shows unambiguous evidence of the light-controlled generation of NO and $^1O_2$. Indeed, we observed the linear photogeneration of NO, which promptly stopped when the light was turned off and restarted as the light was turned on again. It is also noteworthy that the rate of NO release in the nanoassembly is comparable to that obtained for the NO photodonor within the NPs in the absence of porphyrins, indicating that the porphyrin units do not quench the photoexcited NO donor. In addition, we observed the characteristic infrared luminescence of $^1O_2$, decaying by first-order kinetics with a lifetime of approximately 4 μs.

To validate the feasibility of using the bichromophoric nanoassembly for dual-function phototherapeutic activity, cancer cells were incubated for 1 h under different experimental conditions and either kept in the dark or irradiated with visible light for 30 min. The results illustrated in Figure 4 show that only irradiation of the photoactive components in the presence of the CD-based NPs leads to successful photomortality of the cells, thus confirming the photodynamic effects.[29] No significant cell death was detected

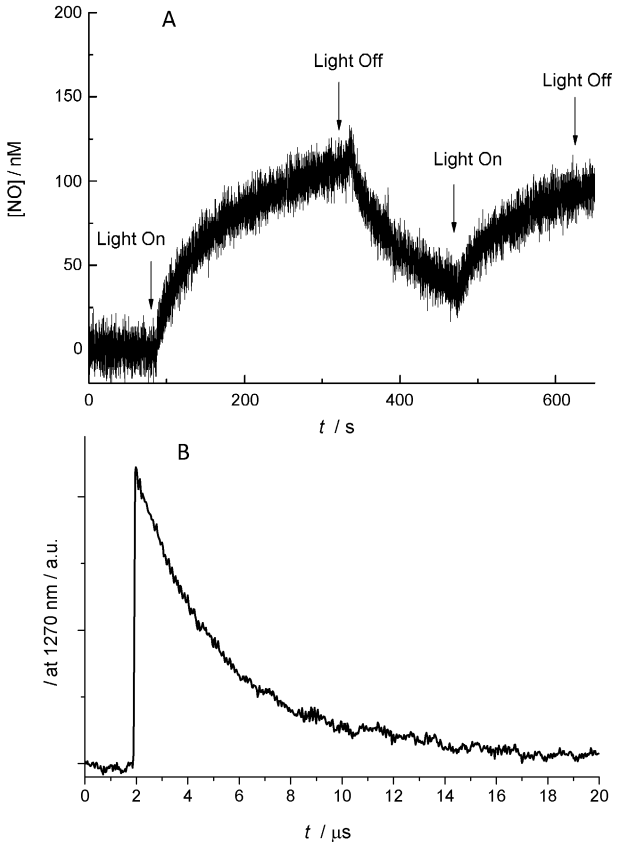

Figure 3. A) NO released upon light irradiation (400 nm) of the bichromophoric CD-based nanoassembly, and B) representative kinetic trace of $^1O_2$ generated upon laser excitation (532 nm). Phosphate buffer (10 mM, pH 7.4), [**1**] = 40 μM, [**2**] = 0.8 μM, [**3**] = 10 μM, T = 25 °C.

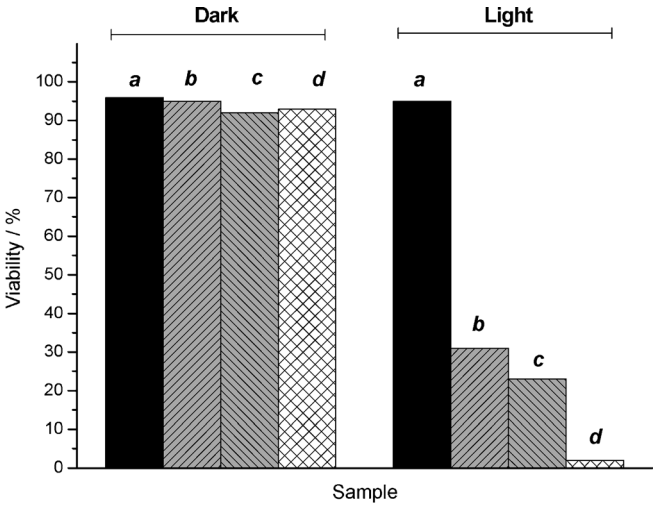

Figure 4. Cell viabilities of HeLa cells incubated with the NPs based on CD **1** (40 μM): ***a***) without the photoactive components and loaded with ***b***) **2** (0.8 μM), ***c***) **3** (10 μM), and ***d***) **2**+**3**.

in the cells that were incubated in the dark or in the absence of the photoactive compounds, indicating a good biocompatibility of the CD-based NPs. The almost complete photody-

namic inactivation induced by the bichromophoric nanoassembly—approximately 98%—in relation to the value observed with the NPs loaded with the single components **2** or **3** provides clear-cut evidence of the involvement of a double-action photoinactivation mechanism in the cell death, in which NO and $^1O_2$ are believed to play a key role.

Conclusion

We have developed a multifunctional photoactive nanoassembly that exploits the different affinities of a $^1O_2$ photosensitizer and a tailor-made NO photodonor towards different compartments in CD-based NPs. Both guests constitute independent photoactive centers, as demonstrated by the preservation of their photophysical and photochemical properties after confinement within the NPs network. We would like to stress that this finding, in contrast with the case of non-photoresponsive compounds, is not obvious. In most cases, in fact, the photoresponse of single or multiple photoactive units located in a confined space can be considerably affected by the occurrence of competitive photoprocesses (e.g., photoinduced energy and/or electron transfer, hydrogen abstraction, nonradiative deactivation, etc.),[30] which preclude the final goal.

We have demonstrated that the fluorescence emission of the porphyrin units allows the localization of the nanoassembly in living cells and provides the bichromophoric system with the ability to generate $^1O_2$ and NO effectively and concurrently, resulting in an amplified level of cancer cell mortality. To the best of our knowledge this is the first report in which cancer cellular death due to the combined action of these two transient species has been shown. The uniting of the dual photodynamic action and the imaging capacities in one single nanostructure, together with its biocompatibility, make this supramolecular architecture an appealing candidate for applications in biomedical research. We finally envision that the extension of our results to a variety of $^1O_2$ and NO photodispensers chosen ad hoc might open fascinating possibilities for novel classes of light-activated, nanoscaled systems in the emerging field of nanomedicine, for multimodal therapy.

Experimental Section

Materials: CD **1** and the model compound **4** were synthesized by the previously reported procedures.[16b,31] The tetraanionic porphyrin **2** was purchased from Sigma–Aldrich and used as received. All other reagents were of the highest commercial grade available and used without further purification. All solvents used (Carlo Erba) were analytical grade.

Syntheses: The synthesis of [7-(adamantan-1-yloxy)heptyl]-[4-nitro-3-(trifluoromethyl)phenyl]amine (**3**) was carried out in two steps. Syntheses were carried out at low light intensity levels.

*1-(7-Bromoheptyloxy)adamantane (**3a**)*: A THF solution of adamantanol (1 g, 6.56 mmol) was added at 0°C under argon to a suspension of sodium hydride (377 mg, 9.84 mmol) in dry THF (10 mL). After the mixture had been left at room temperature for 2 h, 1,7-dibromoheptane (3.92 mL, 22.96 mmol) was added. The reaction mixture was stirred overnight at room temperature and afterwards the excess of NaH was quenched by addition of water. The mixture was concentrated under reduced pressure and the aqueous phase was extracted with Et_2O (3× 10 mL). The organic phases were then collected, washed, dried with Na_2SO_4, filtered, concentrated under reduced pressure, and purified by column chromatography (dichloromethane/cyclohexane 30:70) to give **3a** (yield 90%). ^{1}H NMR ($CDCl_3$, 500 MHz): $\delta = 3.56$ (d, $J = 6.50$ Hz, 2H), 3.26 (t, $J = 6.68$ Hz, 2H), 1.90–1.84 (m, 3H), 1.72–1.35 ppm (m, 24H).

*[7-(Adamantan-1-yloxy)heptyl]-[4-nitro-3-(trifluoromethyl)phenyl]amine (**3**)*: A mixture of **3a** (1 g, 3.03 mmol) and 4-nitro-3-(trifluoromethyl)aniline (200 mg, 1.01 mmoli) was heated at reflux in acetonitrile for 5 days. The organic mixture was dried under vacuum and purified by column chromatography (dichloromethane/cyclohexane 70:30) to afford compound **3** as a yellowish powder (yield 60%). ^{1}H NMR ($CDCl_3$, 500 MHz): $\delta = 7.95$ (d, $J = 9.2$ Hz, 1H), 6.80 (d, $J = 2.4$ Hz, 1H), 6.56 (dd, $J_1 = 9.2$ Hz, $J_2 = 2.4$ Hz, 1H), 4.47 (broad, 1H), 3.34 (dd, $J_1 = 9.5$ Hz, $J_2 = 6.5$ Hz, 2H), 3.15 (dd, $J_1 = 9.8$ Hz, $J_2 = 6.9$ Hz, 2H), 1.83–1.77 (m, 3H), 1.63–1.57 (m, 6H) 1.44–1.18 ppm (m, 16H).

Instrumentation: UV/Vis absorption and fluorescence spectra were recorded with a Jasco V-560 spectrophotometer and a Fluorolog-2 (mod. F-111) spectrofluorimeter, respectively. Nanoparticle sizes were measured with a dynamic light scattering Horiba LS 550 apparatus fitted with a diode laser (wavelength 650 nm). Fluorescence images were taken with a Biomed fluorescence microscope (Leitz, Wetzlar, Germany).

Sample preparation: NPs based on CD **1** were prepared from stock solutions (180 μM) in $CHCl_3$, which were allowed to evaporate slowly to form thin films. The films were hydrated, sonicated for 20 min at 50°C, and allowed to equilibrate overnight. An aqueous solution of the porphyrin **2** was then added and each sample was adjusted to a final volume of 2 mL with phosphate buffer. Compound **3** was dissolved in acetonitrile and allowed to evaporate slowly to form a thin film. This film was then hydrated with the colloidal solutions of CD **1** either with or without the porphyrin **2**. All the final solutions were allowed to equilibrate overnight at 4°C, sonicated for 15 min, and allowed to equilibrate at room temperature for 20 min.

Laser flash photolysis: All of the samples were excited with the second harmonic of a Nd-YAG Continuum Surelite II-10 laser (532 nm, 6 ns FWHM), in quartz cells with a path length of 1.0 cm. The excited solutions were analyzed with a Luzchem Research mLFP-111 apparatus with an orthogonal pump/probe configuration. The probe source was a ceramic xenon lamp coupled to quartz fiber-optic cables. The laser pulse and the mLFP-111 system were synchronized with a Tektronix TDS 3032 digitizer, operating in pre-trigger mode. The signals from a compact Hamamatsu photomultiplier were initially captured by the digitizer and then transferred to a personal computer, controlled by Luzchem Research software operating in the National Instruments LabView 5.1 environment. The solutions were deoxygenated by bubbling with a vigorous and constant flux of pure argon (previously saturated with solvent). In all of these experiments, the solutions were renewed after each laser shot (in a flow cell of 1 cm optical path), to prevent probable autooxidation processes. The sample temperature was 295 ± 2 K. The energy of the laser pulse was measured at each shot with a SPHD25 Scientech pyroelectric meter.

Singlet oxygen detection: Photogeneration of $^1O_2$ upon laser excitation of the photosensitizer was monitored by luminescence measurements in oxygen-saturated solutions. The near-IR luminescence of singlet oxygen at 1.27 μm (resulting from the forbidden transition $^3\Sigma_g^- \leftarrow {}^1\Delta_g$) was probed orthogonally to the exciting beam with a pre-amplified (low impedance) Ge-photodiode (Hamamatsu EI-P, 300 ns resolution) maintained at −196°C and coupled to a long-pass silicon filter (>1.1 μm) and an interference filter (1.27 μm). The pure signal of $^1O_2$ was obtained as the difference between signals in air- and Ar- saturated solutions. The temporal profile of the luminescence was fitted to a single-exponential decay function with exclusion of the initial portion of the plot, which was affected by scattered excitation light, fluorescence, and the formation profile of singlet oxygen itself.

NO detection: NO release was measured with a World Precision Instrument (ISO-NO meter) fitted with a data acquisition system, and based on direct amperometric detection of NO with short response time (<5 s) and sensitivity range of 1 nM to 20 μM. The analogue signal was digitalized with a four-channel recording system and transferred to a PC. The sensor was accurately calibrated by mixing standard solutions of $NaNO_2$ with H_2SO_4 (0.1 M) and KI (0.1 M) according to Equation (1):

$$4H^+ + 2I^- + 2NO_2^- \rightarrow 2H_2O + 2NO + I_2 \quad (1)$$

Irradiation was performed in a thermostatted quartz cell (1 cm path length, 3 mL capacity) with gentle stirring and use of monochromatic radiation (400 nm) from the fluorimeter described above (mod. F-111) as light sources. NO measurements were carried out with the electrode positioned outside the light path to avoid false NO signals due to photoelectric interference on the ISO-NO electrode.

Experiments with cells: HeLa cells were obtained from the American Type Culture Collection and propagated at 1:6 ratio with Dulbecco's modification of Eagle's Minimal Essential Medium supplemented with FBS (Fetal Bovine Serum, 10%). Samples of cells treated with the different samples of NPs based on CD **1** were placed separately in a cuvette and irradiated with a halogen lamp (Osram) for 30 min. The irradiating beam was filtered through a UV filter (Hoya glass type UV-34, cut-off: 340 nm) to cut the UV component and through a 1 cm cell filled with water to remove the IR component. Before and after irradiation, 8×10^4 cells were placed in 96-well plates with RPMI-1640 medium (100 μL) and incubated in the presence of tetrazolium compound [3-(4,5-dimethylthiazol-2-yl)-5-(3-carboxymethoxyphenyl)-2-(4-sulfophenyl)-2*H*-tetrazolium, inner salt; MTS, Promega] and an electron coupling reagent phenazine methosulfate (PMS) dye (MTS 20 μl per well). After further incubation (1 h), the absorbance was read at 490 nm in a microplate reader (Labsystems Multiskan Bichromatic). The cell viability (%) was calculated with the aid of Equation (2):

$$\text{cell viability } (\%) = [A \text{ (before lamp)} - A \text{ (after lamp)}/A \text{ (before lamp)}] \times 100 \quad (2)$$

in which *A* (sample before lamp) represents measurements from the wells treated with samples before the exposure to the halogen lamp and *A* (sample after lamp) represents measurements from the wells treated with samples after the exposure to the halogen lamp.

Acknowledgements

We thank the Marie Curie Program 237962 CYCLON (FP7-PEOPLE-ITN-2008) for financial support to MC fellow N.K. and funding of the research. Financial support from MIUR (PRIN 2008) is also gratefully acknowledged.

[1] *Dynamic Studies in Biology* (Eds.: M. Goeldner, R. Givens), Wiley-VCH, Weinheim, **2005**.

[2] a) A. P. Pelliccioli, J. Wirz, *Photochem. Photobiol. Sci.* **2002**, *1*, 441; b) A. Momotake, N. Lindegger, E. Niggli, R. J. Barsotti, G. C. R. Ellis-Davies, *Nat. Methods* **2006**, *3*, 35; c) P. Neveu, I. Aujard, C. Benbrahim, T. Le Saux, J.-F. Allemand, S. Vriz, D. Bensimon, L. Jullien, *Angew. Chem.* **2008**, *120*, 3804; *Angew. Chem. Int. Ed.* **2008**, *47*, 3744; d) G. Cosa, M. Lukeman, J. C. Scaiano, *Acc. Chem. Res.* **2009**, *42*, 599; e) N. K. Mal, M. Fujiwara, Y. Tanaka, *Nature* **2003**, *421*, 350; f) C. Park, J. Lim, M. Yum, C. Kim, *Angew. Chem.* **2008**, *120*, 3001; *Angew. Chem. Int. Ed.* **2008**, *47*, 2959.

[3] a) M. De, P. S. Ghosh, V. M. Rotello, *Adv. Mater.* **2008**, *20*, 4225; b) S. S. Agasti, A. Chompoosor, C-C. You, P. Ghosh, C. Kyu Kyu, V. M. Rotello, *J. Am. Chem. Soc.* **2009**, *131*, 5728; c) R. Bhattacharya, P. Mukherjee, *Adv. Drug Delivery Rev.* **2008**, *60*, 1289; d) B. Jang, J.-Y. Park, C.-H. Tung, I.-H. Kim, Y. Choi, *ACS Nano* **2011**, *5*, 1086; e) N. Stephanopoulos, G. J. Tong, S. C. Hsiao, M. B. Francis, *ACS Nano* **2010**, *4*, 6014; f) A. Juzeniene, Q. Peng, J. Mohan, *Photochem. Photobiol. Sci.* **2007**, *6*, 1234; g) S. Sortino, *J. Mater. Chem.* **2012**, *22*, 301.

[4] P. Juzenas, W. Chen, Y. P. Sun, M. A. N. Coelho, R. Generalov, N. Generalova, I. L. Christensen, *Adv. Drug Delivery Rev.* **2008**, *60*, 1600.

[5] a) *Nitric Oxide: Biology and Pathobiology*, 2nd ed. (Ed.: L. J. Ignarro), Elsevier, San Diego, **2010**; b) L. J. Ignarro, *Nitric Oxide Biology and Pathobiology*, 1st ed., Academic Press, San Diego, **2000**, p. 41.

[6] a) L. J. Ignarro, *Angew. Chem.* **1999**, *111*, 2002; *Angew. Chem. Int. Ed.* **1999**, *38*, 1882; b) F. Murad, *Angew. Chem.* **1999**, *111*, 1976; *Angew. Chem. Int. Ed.* **1999**, *38*, 1856; c) R. F. Furchgott, *Angew. Chem.* **1999**, *111*, 1990; *Angew. Chem. Int. Ed.* **1999**, *38*, 1870.

[7] a) D. Fukumura, S. Kashiwagi, R. K. Jain, *Nat. Rev. Cancer* **2006**, *6*, 521; b) W. Xu, L. Z. Liu, M. Loizidou, M. Ahmed, I. G. Charles, *Cell Res.* **2002**, *12*, 311; *Nitric Oxide Donors for Pharmaceutical and Biological Applications* (Eds.: P. G. Wang, T. B. Cai, N. Taniguchi), Wiley-VCH, Weinheim, **2005**.

[8] a) P. C. Ford, *Acc. Chem. Res.* **2008**, *41*, 190; b) D. Ostrowski, P. C. Ford, *Dalton Trans.* **2009**, 10660; c) P. G. Wang, M. Xian, X. Tang, X. Wu, Z. Wen, T. Cai, A. J. Janczuk, *Chem. Rev.* **2002**, *102*, 1091; d) M. J. Rose, N. L. Fry, R. Marlow, L. Hinck, P. K. Mascharak, *J. Am. Chem. Soc.* **2008**, *130*, 8834.

[9] Q. Jia, A. Janczuk, T. Cai, M. Xian, Z. Wen, P. G. Wang, *Expert Opin. Ther. Pat.* **2002**, *12*, 819.

[10] a) I. J. MacDonald, T. J. Doughery, *J. Porphyrins Phthalocyanines* **2001**, *5*, 105; b) *Cancer Medicine*, 5th ed. (Eds.: J. F. Holland, E. Frei, III), Decker BC, Ontario, **2000**.

[11] a) R. Pandey, G. Zheng in *The Porphyrin Handbook, Vol. 6* (Eds.: K. Kadish, K. M. Smith, R. Guilard), Academic Press, San Diego, **2000**, pp. 157–230; b) D. K. Chatterjee, L. S. Fong, Y. Zhang, *Adv. Drug Delivery Rev.* **2008**, *60*, 1627.

[12] R. Cai, Y. Kubota, T. Shuin, H. Sakai, K. Hashimoto, A. Fujishima, *Cancer Res.* **1992**, *52*, 2346.

[13] K. J. Reeves, M. W. R. Reed, N. J. Brown, *J. Photochem. Photobiol. B* **2009**, *95*, 141.

[14] a) M. Ferrari, *Nat. Rev. Cancer* **2005**, *5*, 161; b) G. M. Whitesides, *Small* **2005**, *1*, 172; c) M. Eaton, *Nat. Mater.* **2007**, *6*, 251; d) C. A. Strassert, M. Otter, R. Q. Albuquerque, A. Höne, Y. Vida, B. Maier, L. De Cola, *Angew. Chem.* **2009**, *121*, 8070; *Angew. Chem. Int. Ed.* **2009**, *48*, 7928; A. Burns, H. Ow, U. Wiesner, *Chem. Soc. Rev.* **2006**, *35*, 1028; e) M.-R. Choi, K. J. Stanton-Maxei, J. K. Stanley, J. C. S. Levin, R. Bardhan, D. Akin, S. Badve, J. Sturgis, J. P. Robinson, R. Bashir, N. J. Halas, S. E. Clare, *Nano Lett.* **2007**, *7*, 3759; f) S. Wang, R. Gao, F. Zhou, M. Selke, *J. Mater. Chem.* **2004**, *14*, 487.

[15] J. Szejtli, *Chem. Rev.* **1998**, *98*, 1743.

[16] a) P. Falvey, C. W. Lim, R. Darcy, T. Revermann, U. Karst, M. Giesbers, A. T. M. Marcelis, A. Lazar, A. W. Coleman, D. N. Reinhoudt, B. J. Ravoo, *Chem. Eur. J.* **2005**, *11*, 1171; b) R. Donohue, A. Mazzaglia, B. J. Ravoo, R. Darcy, *Chem. Commun.* **2002**, 2864 and references therein.

[17] A. Mazzaglia, N. Micali, L. Monsù Scolaro, M. T. Sciortino, S. Sortino, V. Villari, *J. Porphyrins Phthalocyanines* **2010**, *14*, 661.

[18] a) A. Mazzaglia, N. Angelini, R. Darcy, R. Donohue, D. Lombardo, N. Micali, M. T. Sciortino, V. Villari, L. Monsù Scolaro, *Chem. Eur. J.* **2003**, *9*, 5762; b) A. Mazzaglia, N. Angelini, D. Lombardo, N. Micali, S. Patanè, V. Villari, L. Monsù Scolaro, *J. Phys. Chem. B* **2005**, *109*, 7258.

[19] S. Sortino, A. Mazzaglia, L. Monsù Scolaro, F. Marino Merlo, V. Valveri, M. T. Sciortino, *Biomaterials* **2006**, *27*, 4256.

[20] F. L. Callari, A. Mazzaglia, L. Monsù Scolaro, L. Valli, S. Sortino, *J. Mater. Chem.* **2008**, *18*, 802.

[21] S. Sortino, *Chem. Soc. Rev.* **2010**, *39*, 2903 and references therein.

[22] a) E. B. Caruso, S. Petralia, S. Conoci, S. Giuffrida, S. Sortino, *J. Am. Chem. Soc.* **2007**, *129*, 480; b) S. Conoci, S. Petralia, S. Sortino, *U. S. Pat. Appl. Publ.*, **2009**, pp. 20, Appl. No. PCT/IT2006/000575.

[23] S. Sortino, S. Giuffrida, G. De Guidi, R. Chillemi, S. Petralia, G. Marconi, G. Condorelli, S. Sciuto, *Photochem. Photobiol.* **2001**, *73*, 6.
[24] S. Sortino, G. Marconi, G. Condorelli, *Chem. Commun.* **2001**, 1226.
[25] M. Rekharsky, Y. Inoue, *Chem. Rev.* **1998**, *98*, 1875.
[26] Incorporation of the adamantane moiety into the CD cavity of similar types of amphiphilic CDs has been already reported, see for example: a) J. Voskuhl, M. C. A. Stuart, B. J. Ravoo, *Chem. Eur. J.* **2010**, *16*, 2790; b) B. J. Ravoo, J.-C. Jacquier, G. Wenz, *Angew. Chem.* **2003**, *115*, 2112; *Angew. Chem. Int. Ed.* **2003**, *42*, 2066.
[27] The slight difference of the fluorescence intensity is due to the slight different fractions of absorbed photons by the two samples at the excitation wavelength.
[28] F. Wilkinson, W. P. Helman, A. B. Ross, *J. Phys. Chem. Ref. Data* **1993**, *22*, 113.
[29] Experiments carried out incubating the cancer cells with either the porphyrin **2** or the model compound **4** in the absence of CD NPs showed photoinduced mortality below 5%.
[30] a) S. Monti, S. Sortino, *Chem. Soc. Rev.* **2002**, *31*, 287; b) P. Bortolus, S. Monti, *Adv. Photochem.* **1996**, *22*, 1; V. Ramamurthy, *Photochemistry in Organized and Constrained Media*, Wiley, New York, **1991**.
[31] F. Callari, S. Sortino, *Chem. Commun.* **2008**, 1971.

Received: May 27, 2011
Revised: September 7, 2011
Published online: December 30, 2011

